Theoretical Study of the Structure and Energetics of Silver Clusters

ARTICLE *in* THE JOURNAL OF PHYSICAL CHEMISTRY C · AUGUST 2007

Impact Factor: 4.77 · DOI: 10.1021/jp0717342

3 AUTHORS:

Denitsa Eckweiler
Helmholtz Centre for Infection Research
26 PUBLICATIONS **292** CITATIONS
SEE PROFILE

Valeri G. Grigoryan
Universität des Saarlandes
30 PUBLICATIONS **419** CITATIONS
SEE PROFILE

Michael Springborg
Universität des Saarlandes
266 PUBLICATIONS **2,741** CITATIONS
SEE PROFILE

Theoretical Study of the Structure and Energetics of Silver Clusters

Denitsa Alamanova,† Valeri G. Grigoryan,† and Michael Springborg*

Physical and Theoretical Chemistry, University of Saarland, 66123 Saarbrücken, Germany

Received: March 2, 2007; In Final Form: June 4, 2007

Using four different model potentials for silver, we have calculated the structural and energetic properties of the three energetically lowest isomers of Ag_N clusters. With two versions of the Gupta potential, we have considered N up to 150, whereas clusters with N up to 60 were studied with two different embedded-atom potentials. The results are compared with more accurate theoretical results for small Ag_N clusters and with experimental trapped ion electron diffraction data. It is found that the different potentials lead to related structural patterns, but the structures differ in details. In particular, the model potentials tend to prefer a decahedral growth, whereas experiment suggests icosahedral growth. Moreover, a comparison with related results for other metal clusters is made, too. Here, significant differences to gold clusters are found, and the largest similarity is found when comparing with copper clusters. Clusters of nickel seem to be less similar than copper but more than gold. To quantify these comparisons, various specifically developed descriptors are applied.

I. Introduction

The unique properties of the smallest metal particles, because of their large surface-to-volume atoms ratio, have made them attractive candidates for applications in, for example, the fields of controlled growth of nanostructures, colloidal chemistry, and catalysis. The properties of the clusters depend critically and in a complicated way on the number of atoms, and therefore many different spectroscopic and microscopic techniques have been applied to unravel the structure−property relations of clusters. Here, in particular alkali and coinage metal clusters have been the subject of an intensive research activity (see, e.g., ref 1).

In the present work, we shall focus on silver clusters that have been the subject of many experimental studies.[2−17] None of these has, however, been able to determine unambiguously the structure of the clusters. Only one study[18] on the Raman spectrum of Ag_5 revealed that the molecule has a planar trapezoidal structure.

The fact that the calculation of any property has to rely on an accurate determination of the structure of the lowest total energy together with the rapidly increasing computational demands both in calculating the total energy for any structure and in determining the lowest total energy as a function of cluster size makes it difficult to apply theoretical methods in calculating experimentally accessible properties. Nevertheless, much theoretical effort has been devoted to the determination of the accurate lowest-energy structures as well as optical and conductive properties of small clusters. Several first-principles calculations[19−26] have found that Ag_6 is the largest planar cluster, whereas according to tight-binding calculations[27] the smallest three-dimensional cluster is found for Ag_5. However, both approaches observe an odd−even energy oscillation in the total energy, as also determined by experiment.[2,3] On the other hand, according to the spherical jellium model[28,29] particularly stable cluster sizes should be found for clusters with 2, 8, 18, 20, 40, etc. atoms when assuming that Ag has one valence electron per atom. But a recent[30] density functional study on Ag clusters with 9−20 atoms found that layered structures are the lowest-energy isomers for clusters with less than 16 atoms, while the larger ones are compact with quasispherical shape.

Completely unbiased geometry optimization using ab initio methods are still computationally unfeasible for systems with more than 10−20 atoms. Consequently, beyond that size range one has to obtain structural information with the help of (semi-)empirical potentials that then have to be checked against other theoretical or experimental information. In some cases, these are combined with molecular dynamics techniques so that static and/or dynamical properties can be investigated.[31−37] For instance, using the embedded atom potential (EAM) it has been found that for clusters with up to 23 atoms the structure is based on icosahedral packing, and therefore they exhibit similar thermodynamic behavior. For larger clusters with up to 147 atoms, Garca González and Montejano-Carrizales[38] used the EAM method to compare clusters with different structural motifs, so that no complete structure-optimization was carried through. Even larger silver clusters have been considered by Baletto and co-workers[39−41] who studied the growth of these systems. It was found that the structure of the clusters depends critically on the temperatures at which the growth takes place. By comparing three main structural motifs, that is, icosahedral, decahedral, and (truncated) octahedral structures, they found that icosahedra were favored for small ($N \leq 147$), decahedra for intermediate ($300 \leq N \leq 20\,000$), and octahedra for large sizes ($N > 30000$). A similar trend was observed by Calvo and Doye[42] in a study on the pressure effects on cluster growth. But in none of these studies a systematic determination of the structure of the clusters was undertaken.

On the other hand, this was the case for the studies of Michaelian et al.[43] who used the Gupta potential and for that of Doye and Wales[44] who used the Sutton-Chen potential for unbiased structure optimizations of metal clusters with up to about 80 atoms. Also one of the most recent studies of this

* Corresponding author. E-mail: m.springborg@mx.uni-saarland.de.
† E-mail: (D.A.) deni@springborg.pc.uni-sb.de; (V.G.G.) vg.grigoryan@mx.uni-saarland.de.

10.1021/jp0717342 CCC: $37.00
Published on Web 08/03/2007

TABLE 1: Parameters in the Two Versions of the Gupta Potential Used Here

parameter	tight-binding[47]	second order[48]
A/eV	0.09944	0.1028
p	10.12	10.928
q	3.37	3.139
r_0/Å	1.0	2.892
ζ /eV	1.0	1.178

type, by Shao et al.,[45] used a Gupta potential to study the structures of Ag clusters with up to 80 atoms.

We shall here present results of a theoretical study of the properties of Ag_N clusters with up to 150 atoms using two different versions of the many-body Gupta potential[46] and, moreover, using two different versions of the EAM potential for N up to 60. We shall compare the results from the different approximate descriptions of the interatomic interactions, both with each other and with those of the parameter-free studies and with experimental information. Thereby, we shall discuss to which extent these are reliable in describing the properties of these very small systems, that after all may differ from their macroscopic counterpart, crystalline Ag. In addition, we shall focus on the development of structure and energetics with N for the different potentials.

The paper is organized as follows: in Section II, our theoretical and computational methods are briefly described, and in Section III we present our results. Finally, in Section IV, a brief summary is presented.

II. Methods

The Gupta potential[46] has been derived from Gupta's expression for the cohesive energy of a macroscopic, metallic material and can be written in terms of repulsive and attractive many-body terms

$$E_{\text{tot}} = \sum_{i=1}^{N} \{V^r(i) - V^m(i)\} \tag{1}$$

where

$$V^r(i) = \sum_{j=1(\neq i)}^{N} A \exp\left[-p\left(\frac{r_{ij}}{r_0} - 1\right)\right] \tag{2}$$

and

$$V^m(i) = \left\{\sum_{j=1(\neq i)}^{N} \zeta^2 \exp\left[-2q\left(\frac{r_{ij}}{r_0} - 1\right)\right]\right\}^{1/2} \tag{3}$$

The summations run over all (N) atoms of the system of interest. Furthermore, r_{ij} is the distance between atoms i and j, and A, r_0, ζ, p, and q are fitted to experimental values of the cohesive energy, lattice parameters, and elastic constants for the crystal at 0 K. We have considered two parametrizations, both given in Table 1. Notice, however, that the tight-binding version (TBG) from refs 43 and 47 uses reduced units for the energy and the coordinates, that is, the parameters r_0 and ζ are set equal to 1. It has, however, been emphasized[43] that the unscaled values depend on the system size, N, making it nontrivial to compare the results from this potential with those of the EAM and the extended version of the Gupta potential[48] (nG). To make a direct comparison possible, we determine for each structure that we have obtained with the TBG method separately the scaling factor of the nuclear coordinates (which typically is around 3) that gives the lowest total energy when using the nG potential for that structure. Moreover, the energy from the nG potential is then used as the unscaled energy.

TABLE 2: The Bond Length (in Å) of Ag_2 as Calculated with the Tight-Binding Gupta, the Extended Gupta Potential, and the DBF and VC EAM Potentials[a]

system	nG	TB	VC	DBF	LDA[25]	exp[52,53]
Ag_2	2.449	2.382	2.501	2.443	2.49	2.53

[a] The dimer bond length obtained in reduced units is appropriately scaled. The results are compared to the LDA and experimental values.

For clusters with up to $N = 60$ atoms, we also applied the embedded atom method (EAM). Here, we use both the original version of Daw, Baskes, and Foiles[49] (DBF) and the later version of Voter and Chen[50] (VC). In the latter, the values of the parameters that enter the potential have been obtained by comparing also to properties of the dimer. In both versions, the total energy of the system is split into a sum of atomic energies

$$E_{\text{tot}} = \sum_{i=1}^{N} E_i \tag{4}$$

with

$$E_i = F_i(\rho_i^h) + \frac{1}{2}\sum_{j\neq i}^{N} \phi_{ij}(r_{ij}) \tag{5}$$

The embedding energy F_i is obtained by considering each atom as an impurity embedded into a host provided by the rest of the atoms, whereas the electron−electron interactions ϕ_{ij} are represented through short-ranged pair potentials. Moreover, ρ_i^h is the local electron density at site i, and r_{ij} is the interatomic distance.

Finally, for the determination of the structures of the global total-energy minima we have used our own unbiased Aufbau/Abbau method that is described elsewhere.[51]

III. Results

A. Structural Properties. To check the accuracy of the approximate methods, we first calculated the dimer bond length and compared the results to accurate theoretical and experimental values. As can be seen from Table 2, all approaches provide a fairly accurate description of the structure of the smallest possible cluster. Because only the VC method has incorporated information from the dimer in the parametrization, the agreement is remarkable.

Having estimated the accuracy of the different approaches, we proceed to the structures of all our globally optimized clusters. The symmetries of these structures and the energetically next two isomers with N up to 60 as found with all different theoretical approaches are shown in Table 3 and for $61 \leq N \leq 150$ from the calculations with the Gupta potentials in Table 4. In previous studies, we have optimized the structures of nickel,[51] copper,[54] and gold clusters[55] with up to 150 atoms using the DBF and VC EAM potentials. We found that the two EAM methods provide very similar structures for the smallest nickel and copper clusters, but that some differences showed up for the smallest gold clusters making the applicability of these methods to the properties of gold clusters somewhat questionable.[56]

The smallest clusters for which different structures are found for different methods occur for $N = 15$. In this case, the high-symmetric D_{6d} structure (which is the one of the global total-energy minimum for Cu_{15}) is the second isomer according to

TABLE 3: The Point Groups of the Ag_N Clusters for $2 \leq N \leq 60$ as Obtained with the Different Parametrized Potentials[a]

N	*N*.1	*N*.2	*N*.3	N	*N*.1	*N*.2	*N*.3	N	*N*.1	*N*.2	*N*.3
				21	C_1/C_1	C_1/C_1	C_{2v}/D_2	41	C_s/D_2	C_{3v}/C_{3v}	C_{3v}/C_{3v}
					C_s/C_1	C_1/C_s	C_2/C_s		C_1/C_s	C_3/C_s	C_s/C_1
2	$D_{\infty h}/D_{\infty h}$			22	C_s/C_s	C_1/C_1	D_{6h}/D_{6h}	42	C_s/C_s	C_s/C_1	C_{2v}/C_1
	$D_{\infty h}/D_{\infty h}$				C_s/C_1	D_{6h}/C_s	C_1/C_s		C_{2v}/C_s	C_s/C_s	C_1/C_1
3	D_{3h}/D_{3h}			23	C_2/D_2	D_{3h}/C_s	C_s/C_s	43	C_s/C_1	C_{2v}/C_s	C_1/C_s
	D_{3h}/D_{3h}				D_{3h}/D_{3h}	C_2/C_2	D_{3h}/C_s		C_s/C_s	C_1/C_s	C_1/C_1
4	T_d/T_d			24	C_s/C_s	C_s/D_2	C_2/C_s	44	C_s/C_s	C_1/C_1	C_s/C_1
	T_d/T_d				D_3/C_{2v}	C_{2v}/C_s	C_s/D_3		C_s/C_1	C_2/C_s	C_s/C_1
5	D_{3h}/D_{3h}			25	C_3/C_3	C_{3v}/C_1	C_{2v}/C_1	45	C_s/C_1	C_s/C_s	C_1/C_1
	D_{3h}/D_{3h}				C_3/C_3	C_1/C_s	C_{2v}/C_1		C_s/C_s	C_s/C_s	C_s/C_1
6	O_h/O_h	C_{2v}/C_{2v}		26	C_1/C_1	D_{3h}/C_{2v}	C_{2v}/C_s	46	C_{2v}/C_s	C_1/C_1	C_1/C_1
	O_h/O_h	C_{2v}/C_{2v}			C_1/C_1	C_{2v}/T_d	C_s/C_{2v}		C_{2v}/C_{2v}	C_1/C_1	C_s/C_1
7	D_{5h}/D_{5h}	C_{3v}/C_{3v}	C_2/C_2	27	C_s/C_s	C_2/C_2	C_1/C_1	47	C_1/C_1	C_s/C_1	C_s/C_1
	D_{5h}/D_{5h}	C_{3v}/C_{3v}	C_2/C_2		C_s/C_s	C_s/C_s	C_2/C_2		C_1/C_1	C_1/C_s	C_s/C_s
8	D_{2d}/D_{2d}	C_s/C_s	D_{3d}/D_{3d}	28	C_1/D_2	T/C_s	C_s/C_1	48	D_2/D_2	C_s/C_1	C_s/C_s
	D_{2d}/D_{2d}	C_s/C_s	D_{3d}/D_{3d}		T/T	C_1/C_1	C_s/C_{3v}		C_{2v}/C_s	C_s/C_s	C_s/C_{2v}
9	C_{2v}/C_{2v}	D_{3h}/C_{3v}	C_{2v}/C_s	29	C_3/C_2	C_2/C_s	C_s/C_2	49	C_{3v}/C_{3v}	C_s/C_1	C_s/C_1
	C_{2v}/C_{2v}	D_{3h}/D_{3h}	C_1/C_{2v}		C_3/C_3	C_{2v}/C_{2v}	C_s/C_2		C_{3v}/C_{3v}	C_s/C_s	C_1/C_1
10	C_{3v}/C_{3v}	D_{2h}/D_{2h}	C_2/C_2	30	C_s/C_s	C_{2v}/C_1	C_1/C_1	50	C_s/C_s	C_s/C_s	C_s/C_s
	C_{3v}/C_{3v}	D_{2h}/D_{2d}	D_{4d}/D_{2h}		C_s/C_s	C_1/C_{2v}	C_1/C_1		C_s/C_s	C_{2v}/C_s	C_1/C_s
11	C_{2v}/C_{2v}	C_2/C_2	C_{2v}/C_2	31	C_{2v}/C_3	C_3/C_s	C_{2v}/D_2	51	C_s/C_s	C_s/C_s	C_1/C_1
	C_{2v}/C_{2v}	C_2/C_2	C_{2v}/C_2		C_3/C_s	C_s/C_1	C_1/C_s		C_{2v}/C_s	C_s/C_s	C_s/C_1
12	C_{5v}/C_{5v}	D_{2d}/D_{2d}	D_{3h}/D_{3h}	32	D_{2d}/D_{2d}	C_{2v}/C_{2v}	C_2/C_3	52	C_{2v}/C_{2v}	C_s/C_{3v}	C_s/D_2
	C_{5v}/C_{5v}	C_1/D_{2d}	D_{3h}/C_1		D_3/C_{2v}	D_{2d}/D_3	C_{2v}/T_h		C_{3v}/C_{2v}	C_s/C_{3v}	C_s/C_s
13	I_h/I_h	C_s/C_s	C_s/C_1	33	C_{2v}/C_s	C_1/C_2	C_s/C_{2v}	53	C_{2v}/C_{5v}	C_{2v}/D_2	C_{5v}/D_{5d}
	I_h/I_h	C_s/C_s	C_s/C_s		C_2/C_2	C_s/C_s	C_s/C_1		C_{2v}/C_{2v}	D_{5d}/D_{5d}	C_{2v}/C_{2v}
14	C_{3v}/C_{3v}	C_{2v}/C_{2v}	C_{6v}/C_2	34	C_s/C_2	C_s/D_2	C_s/C_s	54	C_{5v}/I_h	I_h/C_{5v}	C_{2v}/D_2
	C_{3v}/C_{3v}	C_{2v}/C_{2v}	C_{6v}/C_1		C_s/C_s	C_s/C_s	C_1/C_1		C_{5v}/C_{5v}	I_h/I_h	C_{2v}/C_{2v}
15	C_{2v}/D_{6d}	D_{6d}/C_{2v}	C_{2v}/C_{2v}	35	C_s/D_3	D_3/C_s	C_{2v}/D_2	55	I_h/I_h	C_1/C_s	C_s/C_1
	D_{6d}/C_{2v}	C_{2v}/D_{6d}	C_{2v}/C_{2v}		D_3/D_3	C_{2v}/C_{2v}	C_{2v}/C_1		I_h/I_h	C_1/C_s	C_s/C_1
16	C_s/C_{2v}	C_1/C_1	C_s/C_s	36	C_s/C_2	C_s/C_1	C_2/D_2	56	C_{3v}/C_s	C_s/C_{2v}	C_s/C_{3v}
	C_s/C_s	C_s/C_s	D_{3h}/C_1		C_2/C_1	C_1/C_2	C_s/C_1		C_s/C_{3v}	C_{3v}/C_s	C_{3v}/C_s
17	C_2/C_{2v}	C_2/C_2	C_{2v}/C_s	37	C_{3v}/C_{2v}	C_s/C_{2v}	C_{2v}/C_s	57	C_s/C_{3v}	C_s/C_1	C_s/C_s
	C_2/C_2	C_s/C_s	C_{2v}/C_s		C_{3v}/C_2	D_2/C_{5v}	C_s/C_1		C_s/C_s	C_1/C_s	C_s/C_s
18	C_s/C_2	C_s/C_s	C_2C_{2v}	38	O_h/O_h	C_{5v}/D_{4h}	D_{4h}/D_2	58	C_{3v}/C_{3v}	C_1/C_1	C_1/C_{3v}
	C_s/C_s	C_2/C_{5v}	C_{2v}/C_s		O_h/O_h	D_{4h}/C_{5v}	D_2/C_{5v}		C_{3v}/C_{3v}	C_1/C_1	C_1/C_1
19	D_{5h}/D_{5h}	C_2/C_s	C_s/C_s	39	C_{5v}/D_4	C_{4v}/D_3	C_s/C_s	59	C_{2v}/C_1	C_1/C_{2v}	C_1/C_1
	D_{5h}/D_{5h}	C_1/C_1	C_s/C_s		C_5/C_{5v}	C_{5v}/C_s	C_{4v}/C_s		C_1/C_{2v}	C_{3v}/C_1	C_{2v}/C_1
20	C_{2v}/C_{2v}	D_2/D_2	D_{3d}/D_{3d}	40	C_s/D_{4h}	C_s/D_2	C_1/C_s	60	C_s/C_s	C_s/C_s	C_1/C_1
	C_{2v}/C_{2v}	D_2/D_{3d}	D_{3d}/D_2		C_s/C_s	D_2/C_s	C_2/C_2		C_s/C_s	C_s/C_1	C_s/C_{2v}

[a] *N.k* gives the results for the energetically *k*-lowest isomer of the Ag_N cluster. For each *N*, the first row shows the results from the *n*G/TB Gupta potentials and the second row those for the VC/DBF EAM potentials.

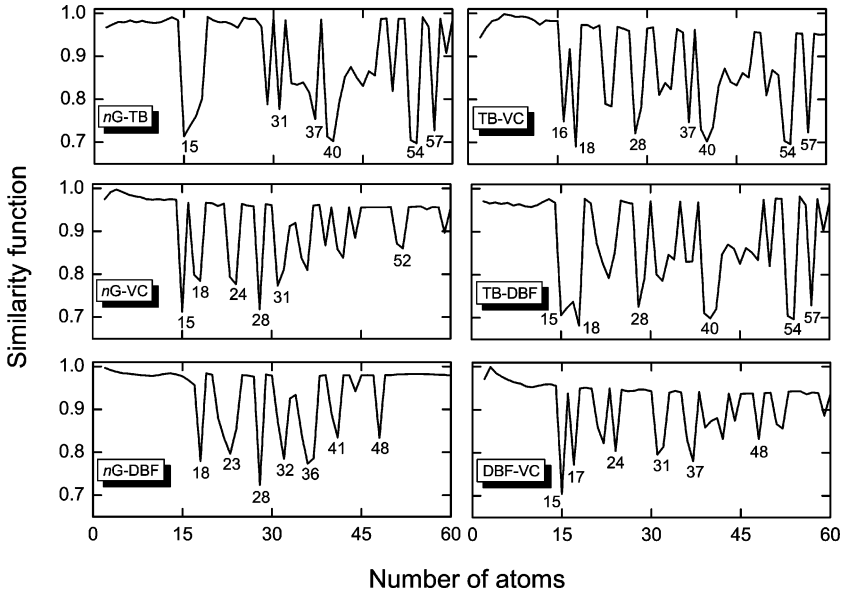

Figure 1. The similarity functions obtained when comparing the global minima structures from the different potentials.

the *n*G and the DBF potentials. A further difference to the results for Cu_N clusters is that the tetrahedral $N = 17$ and $N = 92$ clusters for copper are not among the three lowest-lying isomers for the Ag clusters. Instead, low-symmetrical structures are

TABLE 4: As Table 3 but for 61 ≤ *N* ≤ 150 and Only for the Two Gupta Potentials

N	*N*.1	*N*.2	*N*.3	N	*N*.1	*N*.2	*N*.3	N	*N*.1	*N*.2	*N*.3
61	C_{2v}/C_{2v}	C_s/C_s	C_1/C_s	91	C_1/C_1	C_1/C_1	C_s/C_1	121	C_{2v}/C_{2v}	C_1/C_1	C_1/C_1
62	C_s/C_s	C_1/C_s	C_1/C_1	92	C_1/C_1	C_1/C_1	C_1/C_1	122	C_s/C_s	C_s/C_1	C_1/C_s
63	C_{2v}/C_{2v}	C_1/C_s	C_1/C_1	93	C_1/C_1	C_1/C_1	C_1/C_1	123	C_{2v}/C_{2v}	C_1/C_1	C_1/C_1
64	C_s/C_s	C_1/C_1	C_1/C_1	94	C_1/C_1	C_1/C_1	C_1/C_1	124	C_s/C_s	C_1/C_1	C_1/C_1
65	C_{2v}/C_{2v}	C_1/C_s	C_s/C_1	95	C_1/C_1	C_1/C_1	C_1/C_1	125	C_1/C_1	C_1/C_1	C_1/C_1
66	C_s/C_s	C_s/C_s	C_1/C_1	96	C_1/C_s	C_1/C_1	C_1/C_1	126	C_s/C_s	C_1/C_1	C_1/C_1
67	C_{2v}/C_{2v}	C_s/C_s	C_1/C_1	97	C_2/C_2	C_1/C_1	C_1/C_1	127	C_s/C_s	C_s/C_1	C_s/C_s
68	C_{2v}/C_{2v}	C_s/C_s	C_1/C_1	98	C_s/C_s	T_d/C_1	C_1/C_1	128	C_s/C_s	C_{2v}/C_s	C_1/C_s
69	C_s/C_s	C_1/C_1	C_1/C_1	99	C_s/C_s	C_1/C_1	C_1/C_1	129	C_s/C_s	C_1/C_1	C_1/C_1
70	C_s/C_s	C_1/C_1	C_1/C_1	100	C_{5v}/C_s	C_1/C_1	C_s/C_1	130	C_{2v}/D_2	C_1/C_1	C_1/C_s
71	C_{2v}/C_{2v}	C_1/C_1	C_1/C_1	101	D_{5h}/D_{5h}	C_s/C_s	C_s/C_s	131	C_s/C_s	C_s/C_s	C_s/C_s
72	C_s/C_s	C_1/C_s	C_1/C_1	102	C_s/C_s	C_s/C_s	C_1/C_{2v}	132	C_s/C_s	C_1/C_1	C_1/C_1
73	C_s/C_s	C_s/C_s	C_1/D_{5h}	103	C_{2v}/C_{2v}	C_2/C_s	C_s/D_2	133	C_s/C_s	C_1/C_s	C_1/C_s
74	C_{5v}/C_{5v}	C_1/C_1	C_s/C_s	104	C_1/C_1	C_s/C_1	C_1/C_1	134	C_s/C_s	C_1/C_s	C_1/C_{2v}
75	D_{5h}/D_{5h}	C_s/C_s	C_1/C_s	105	C_{2v}/C_{2v}	C_2/C_{2v}	C_s/C_1	135	C_s/C_s	C_1/C_s	C_s/C_s
76	C_{2v}/C_{2v}	C_s/C_s	C_s/C_s	106	C_1/C_1	C_s/C_s	C_s/C_s	136	C_1/C_1	C_1/C_1	C_1/C_1
77	C_{2v}/C_{2v}	C_1/C_{2v}	C_1/C_{2v}	107	C_{2v}/C_{2v}	C_1/C_{2v}	C_1/C_1	137	C_s/C_s	C_1/C_1	C_1/C_1
78	C_s/C_s	C_s/C_s	C_{2v}/C_{2v}	108	C_1/C_1	C_1/C_1	C_1/C_1	138	C_s/C_s	C_1/C_1	C_1/C_1
79	O_h/O_h	C_1/C_{2v}	C_1/C_{2v}	109	C_1/C_1	C_1/C_1	C_1/C_1	139	C_{2v}/D_2	C_s/C_1	C_{5v}/C_s
80	C_s/C_s	C_1/C_s	C_1/C_s	110	C_1/C_1	C_1/C_1	C_1/C_1	140	C_{5v}/C_s	C_{3v}/O_h	C_{3v}/C_s
81	C_{2v}/C_{2v}	C_s/C_s	C_1/C_s	111	C_1/C_1	C_1/C_1	C_1/C_1	141	C_s/C_s	C_s/C_{2v}	C_s/C_s
82	C_{2v}/C_{2v}	C_s/C_s	C_s/C_s	112	C_1/C_1	C_1/C_1	C_1/C_1	142	C_{2v}/D_2	C_s/C_s	C_s/C_s
83	C_{2v}/C_{2v}	C_s/C_s	C_1/C_{2v}	113	C_s/C_s	C_1/C_1	C_1/C_1	143	C_s/C_{3v}	C_s/C_s	C_s/C_s
84	C_s/C_s	C_{2v}/C_{2v}	C_{2v}/C_s	114	C_1/C_1	C_1/C_1	C_s/C_1	144	C_{2v}/D_2	D_{5d}/I_h	C_{2v}/D_2
85	C_s/C_s	C_s/C_s	C_s/C_s	115	C_s/C_s	C_1/C_s	C_1/C_1	145	C_{5v}/I	C_{2v}/D_2	C_s/D_2
86	C_{2v}/C_{2v}	C_s/C_s	C_s/C_1	116	D_{3d}/T_h	O_h/T	C_1/O_h	146	I_h/I_h	C_{5v}/I	D_{5h}/C_s
87	C_s/C_s	C_s/C_s	C_1/C_s	117	C_1/C_1	C_1/C_1	C_1/C_1	147	I_h/I_h	C_s/C_s	C_s/C_s
88	C_s/C_s	C_s/C_s	C_1/C_s	118	C_1/C_1	C_1/C_1	C_1/C_1	148	C_s/C_s	C_s/C_s	C_s/C_s
89	C_s/C_s	C_1/C_s	C_1/C_1	119	C_1/C_1	C_{2v}/C_{2v}	C_1/C_1	149	C_{3v}/C_{3v}	C_{3v}/D_2	C_s/C_{3v}
90	C_s/C_s	C_1/C_1	C_1/C_1	120	C_s/C_s	C_1/C_1	C_1/C_1	150	C_s/C_s	C_1/C_{3v}	C_1/C_s

found. On the other hand, for $N = 28$ the second isomer of the *n*G potential and the global minima from the VC potential all have the *T* symmetry, as is the case of the Cu_{28} cluster, whereas all isomers found with the TBG potential are disordered. The tetrahedron at $N = 17$ is also the global minimum for the corresponding gold cluster but not for Ni_{17} where the four lowest isomers have low symmetry.

Also, for $N = 38$ all methods find a high-symmetric structure as that of the global total-energy minimum, that is, a truncated octahedron, whereas the second Mackay icosahedron is found for $N = 55$ and the Marks decahedron is found for $N = 75$. These structures are found for other metals, too, with Au being an exception in some cases. Another difference to gold is that the tetrahedral structure that we have found for Au_{34} is not found for any other metal (independent of potential). Highly symmetrical tetrahedral and octahedral structures are among the first three isomers for Ag_{116}, while the global minima structures for copper and nickel have icosahedral symmetry. Finally, an icosahedral-like global minimum is found for the Ag_{140} cluster with the *n*G potential, while for gold it has an octahedral symmetry. However, the equivalent copper and nickel clusters have disordered icosahedral ground-state structures.

Our results for the global minima structures of silver clusters with $N = 6$, 7, 12, 13, 14, 19, 38, 55, and 75 atoms are consistent with those by Michaelian et al.[43] who used the TBG version of the Gupta potential. Up to $N = 22$, our global minima structures obtained with the *n*G potential are identical to those found with the Sutton−Chen potential by Doye and Wales.[44]

To obtain quantitative information on the differences or similarities between two structures, we shall use the concept of similarity functions that we have introduced earlier.[51,54] For each atom of the first cluster we define its radial distance

$$r_n = |\vec{R}_n - \vec{R}_0| \tag{6}$$

with a center

$$\vec{R}_0 = \frac{1}{N}\sum_{j=1}^{N}\vec{R}_j \tag{7}$$

These are sorted in increasing order: $\{r_n\}$ with $r_1 \le r_2 \le r_3 \le ... \le r_N$. In a similar manner, for the second cluster we calculate and sort the radial distances $\{r'_n\}$ too. Subsequently, from

$$q = \left[\frac{1}{N}\sum_{n=1}^{N}(r_n - r'_n)^2\right]^{1/2} \tag{8}$$

a similarity function is defined as

$$S = \frac{1}{1 + q/u_l} \tag{9}$$

($u_l = 1$ Å) which approaches 1 if the two structures are very similar. We shall now use these in comparing the structures from the different potentials, those of different metals, and our results with those of others.

First, we compare the structures we have obtained with the different potentials. The resulting similarity functions are shown in Figure 1. It is clear that only up to *N* around 15 all theoretical methods give roughly the same structures. For the larger values of *N*, the different potentials repeatedly yield different ground-state structures. Certain values, for instance $N = 28$, appear then to be more problematic than others. However, one reason is that small variations in the details of the potentials easily lead to an interchange of the energetic ordering of different isomers, in particular when they are close in energy, leading to markedly different ground-state structures. This is indicated by the results in Table 3 (cf., e.g., the results for $N = 28$). Below,

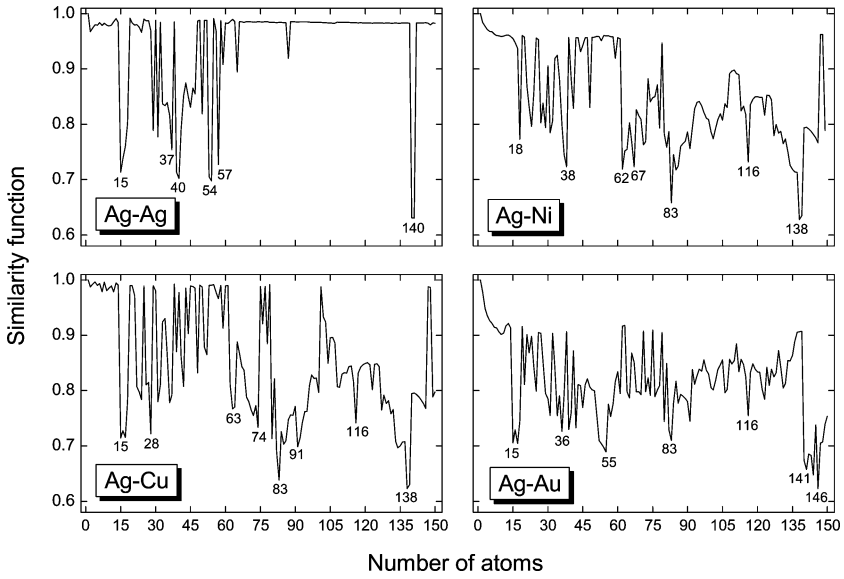

Figure 2. Structural comparison between the silver clusters obtained in this study with the *n*G version of the Gupta potential and Cu_N, Ni_N, and Au_N clusters from our previous works derived using the VC version of the EAM. In the top left panel, we show the results when comparing the two Gupta potentials.

we shall see that in many cases the two energetically lowest isomers are indeed close in energy.

Next, we compare the structures of the Ag clusters with those of other elements, that is, with the structures of copper, nickel, and gold clusters that we have determined in earlier studies.[51,54,55] To compare the structures, we have rescaled the structures according to the lattice constants of the crystalline materials. The resulting similarity functions are shown in Figure 2. We first notice that the larger silver clusters obtained with the two Gupta potentials are more similar than is the case for the smaller ones with up to 60 atoms. The largest structural differences occur at $N = 140$ and 141, where the global minima have icosahedral elements according to the *n*G potential. The next two Ag_{140} isomers obtained with this potential are also icosahedral. On the other hand, the lowest-lying Ag_{140} and Ag_{141} isomers predicted by the TBG potential have decahedral structures. A previous density functional study[57] predicted icosahedral structures for the silver clusters with $N = 55$, 135, and 140 atoms.

When comparing the silver clusters with those of Ni, Cu, and Au, it is clear that Ag clusters structurally resemble much more Cu clusters than Au clusters, at least up to $N \simeq 80$. Above this value, the Ag clusters are structurally quite different from those of the other elements. Finally, the structures of the nickel clusters seem to be in between those of copper and gold, at least in comparison with those of silver clusters.

We shall next compare our calculated structures with the ones found in the density functional study of Yang et al.[30] We will use the similarity functions to compare our optimized structures with those of Yang et al.[30,58] The results are shown in Figure 3. For $N = 4$, 5, and 6, none of the present approaches provides a correct description of the structure of global total-energy minimum. The reason is that the density functional calculations predict that these structures are planar, whereas the model potentials all have a tendency toward close packing. On the other hand, it shall also be remembered that small inaccuracies in the total energy very easily lead to a change in the relative ordering of the energetically lowest structures for a given *N*. Thereby, it may happen that a (semi-)empirical potential finds a structure close to the ground-state structure of density functional calculations as an energetically excited structure.

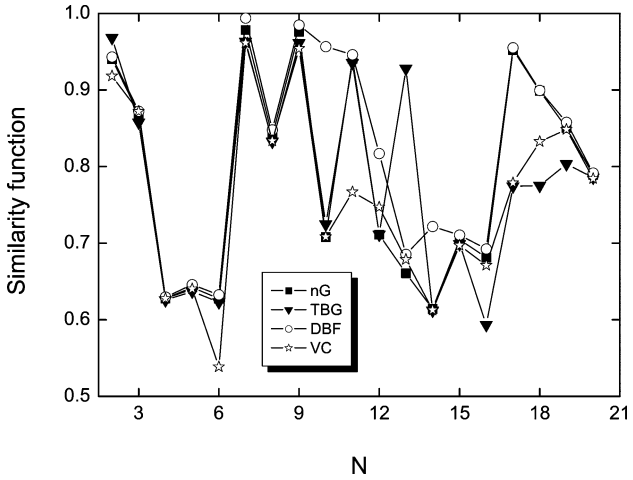

Figure 3. Structural comparison between the silver clusters obtained in this study and those of Yang et al.[30]

Actually, when comparing all the energetically three lowest structures from the model potentials with those of the density functional calculations, a larger value of the similarity function was found in many cases for the second or third isomer than for the first one. Nevertheless, when comparing with the similarity functions in Figures 1 and 2, it is clear that the values in Figure 3 are often low indeed, suggesting that methods that include electronic degrees of freedom find markedly different structures for the absolutely smallest clusters of metal atoms for which approximate methods based on considerations for the infinite metals may be less accurate. The comparison between the two Gupta potentials in Figure 2 suggests, furthermore, that for *N* around roughly 50 these approximate methods may become increasingly accurate.

The discrepancies between the density functional results and our model potential results may be related to the lack of an accurate description of directional, covalent bonds in the latter. For the smallest clusters, such bonds are most likely very important, whereas for extended systems a metallic behavior with delocalized electrons makes an accurate description of such bonds less important. As a further consequence of this problem, the present model potential calculations may tend to produce more compact, closed-packed structures. To analyze this aspect

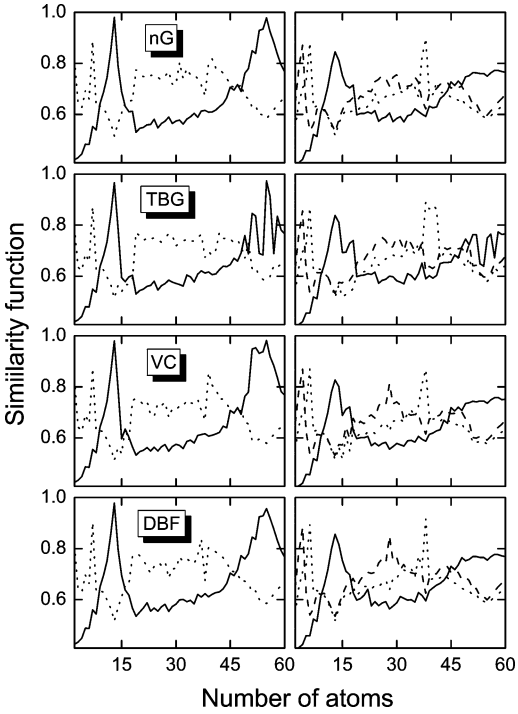

Figure 4. Structural comparison between the silver clusters obtained in this study and fragments of (right panels) an fcc crystal or (left panels) of an icosahedron or decahedron. In the right panels, the different curves correspond to different choices for the center of the spherical cut-out of the crystal (solid curve, the center is at the position of an atom; dashed curve, the center is on the midpoint of a nearest-neighbor bond; dotted curve, the center is at the center of the cubic cell), and in the left panels the solid curve shows the results for the icosahedron and the dotted curve those for the decahedron.

further, we shall compare the optimized structures with the structure of the crystal as well as with a large icosahedron and a large decahedron. To this end, we use again the useful concept of a similarity function defined before via eqs 8 and 9. For each of the reference structures, we choose a center (a large set of radial distances $\{r'_n\}$ is calculated with respect to this center) either the position of an atom, the midpoint of a nearest-neighbor bond, or the center of the cubic unit cell for the face-centered cubic (fcc) lattice, as well as the center for the icosahedron with 147 atoms and the center for the decahedron with 75 atoms.

The results for the similarity function are shown in Figure 4. We see here that for N up to 60 the structures can hardly be described as fragments of the crystal. On the other hand, all our theoretical approaches predict structures that in general have a closer similarity with a decahedron than with an icosahedron, except near those values of N (i.e., 13 and 55) where particularly stable, highly symmetric icosahedra exist.

B. Energetic Properties. In studying energetic properties, we shall first address the question whether the silver clusters are unique or, alternatively, whether they resemble those of other metals. To this end, we scaled our global total-energy minima structures of the copper, gold, and nickel clusters and recalculated their total energies using the *n*G potential for silver. The results can be seen at Figure 5. It is clear that the largest differences are seen for the gold clusters that, indeed, possess markedly different structures from those of the Ag clusters.[55] Among the other two metals, copper seems to be the one energetically and structurally closest to silver. Except for a small size range, $N = 70-80$, the two curves lie very close.

Particularly stable clusters can, for example, be identified through the energetic difference between the first and second

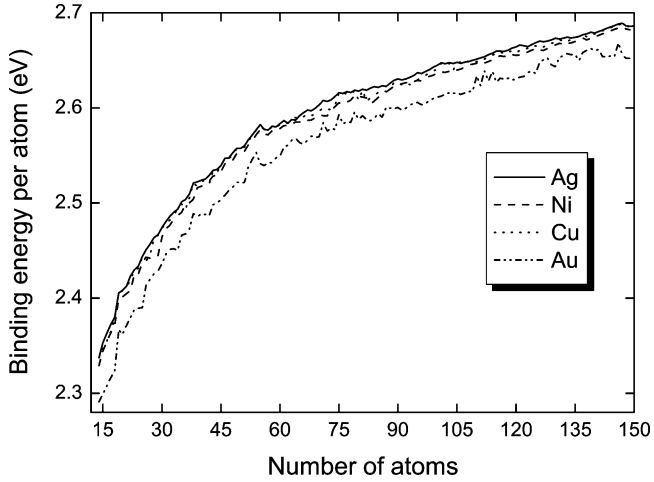

Figure 5. The binding energy per atom for the four different metals after scaling and recalculation of the total energy.

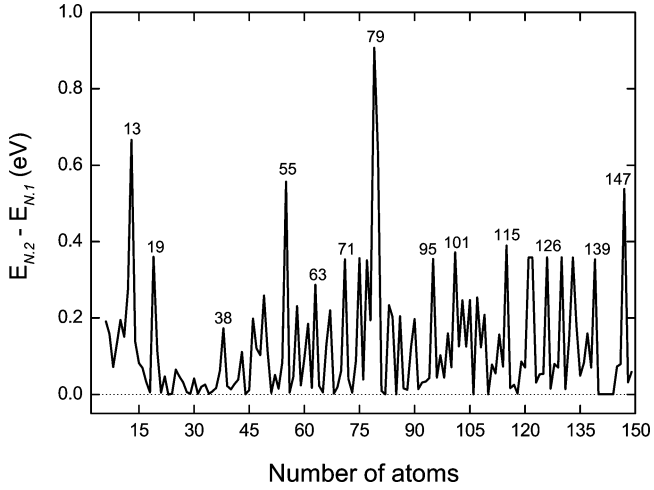

Figure 6. The energetic difference between the two lowest-lying isomers obtained with the *n*G potential.

isomers. This is shown in Figure 6 for the *n*G potential. The results obtained with the TBG potential are not shown, as they are very similar. In the figure, the most pronounced peak is found for the Ag_{79} cluster, but several further peaks are seen. All of these clusters, except for the Ag_{63} and Ag_{79} clusters, have decahedral structures. In contrast to our earlier results for nickel and copper clusters but similar to those for gold clusters, we do not find peaks for $N = 23$, 28, and 137.

Alternatively, the stability function: $E_{tot}(N + 1.1) + E_{tot}(N - 1.1) - 2E_{tot}(N.1)$, where $E_{tot}(N.k)$ is the total energy of the energetically k-lowest isomer of the Ag_N cluster, can also be used in identifying the particularly stable, "magic" clusters. In Figure 7, the stability function for the silver clusters optimized with the *n*G potential is presented. For the sake of comparison with the TBG, DBF, and VC potentials, it is also shown for the size range $N = 2-60$ atoms in Figure 8.

Whereas many of the maxima in Figure 6 are recovered in Figure 7, there are also some differences. Thus, according to Figure 7 the Ag_{23} and Ag_{28} clusters are not particularly stable. Instead, the Ag_{38} and Ag_{61} clusters are found to be magic. In comparison to the results for the copper clusters, the silver clusters with $N = 86$, 92, 116, 119, and 131 are not particularly stable, while the magic Ag_{121} and Ag_{130} are not found for the copper clusters. $N = 116$, 131, and 137 correspond to magic clusters for Ni but not for Ag, whereas the opposite is the case for $N = 95$, 101, 121, 130, and 139. However, the stability

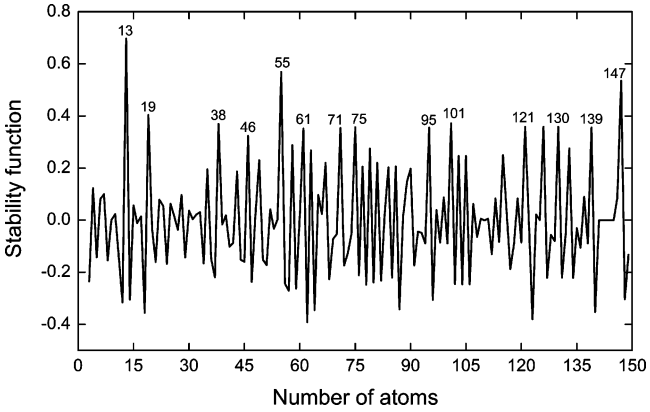

Figure 7. The stability function for the silver clusters obtained with the *n*G potential.

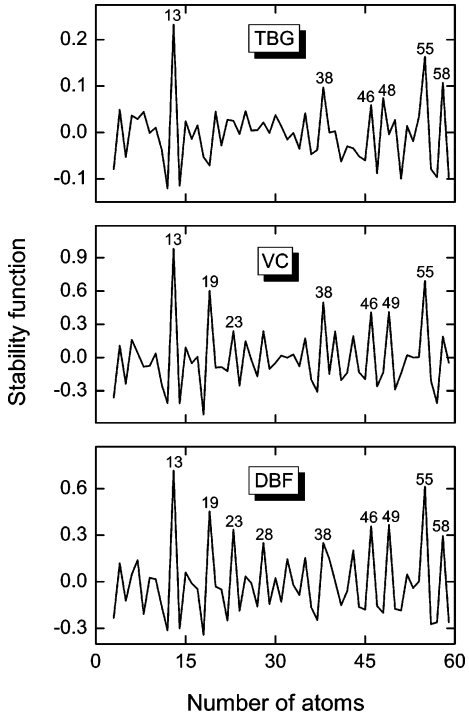

Figure 8. The stability function for silver clusters with up to 60 atoms with three different potentials. Notice the different scalings on the ordinate axes.

functions for these three metals are much more similar than is the case when comparing with the function for gold clusters.

When comparing the different potentials, cf. Figure 8, it is clear that the two EAM methods yield almost the same magic-numbered clusters with increasing stability, and the TB potential gives somewhat different results. Furthermore, the absolute values of the stability function for the different potentials show a suprising scatter, suggesting that the methods hardly agree in absolute values of total-energy variations.

In a recent study, Shao et al.[45] optimized Ag_N clusters with up to 80 atoms using the same (TBG) Gupta potential as we have considered but a different structure optimization method. Their results regarding energetics and structure agree predominantly with ours, although in around 10 cases their total energies are 0.01−0.03 eV lower than ours, in one case about 0.1 eV lower than ours, and in one case theirs is higher than ours. The last case, $N = 79$, is according to our study a particularly stable one but not according to the study of Shao et al. In all the other cases, the clusters do not correspond to particularly stable ones in any of the two studies and are, moreover, of low symmetry.

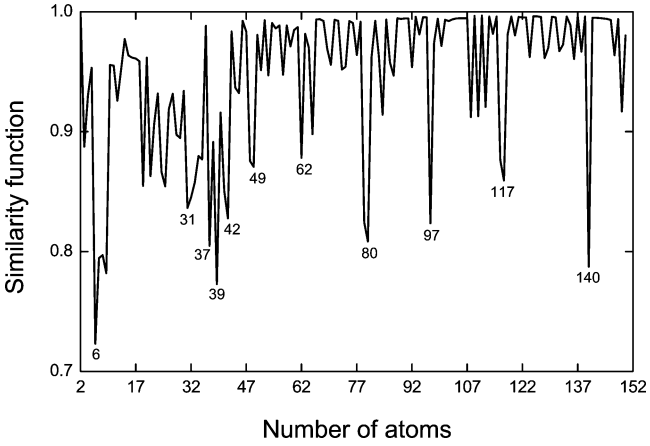

Figure 9. The similarity function for the case when we compare a cluster with N atoms to the $(N - 1)$ atom one plus an extra atom. Only the lowest-lying isomer for each *n*G silver cluster size is considered.

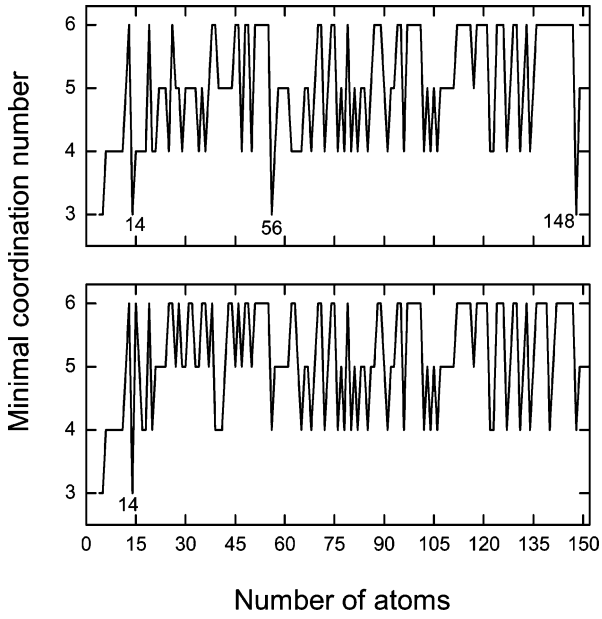

Figure 10. The minimal coordination numbers for the silver clusters obtained with the *n*G (top) and the tight-binding Gupta potential (bottom).

Because of the small total-energy differences between different isomers, (cf. Figure 6), the differences between our results and those of Shao et al. confirm that it is extremely difficult to locate the structures of the global total minima, and that even in the cases where the two studies agree, they may both be wrong!

C. Growth Patterns. Insight into the cluster growth can be obtained by considering how different a cluster with N atoms is from that of $N - 1$ atoms. Once again we use the concept of similarity functions. We consider all the N different structures that can be obtained by removing one of the atoms from the Ag_N cluster. Subsequently, each of those is compared with the Ag_{N-1} cluster and the largest value of S is chosen with S being defined through eqs 8 and 9. The results for the *n*G potential are shown in Figure 9. There are many low values of the similarity function, which indicates an irregular growth of the silver clusters. The small values of S for clusters with up to around 50 atoms have also been found earlier for clusters of nickel[51] and copper.[54] Above this size range, the growth becomes more regular with, however, several structural changes, whose cluster sizes are marked in the figure. According to our results, the cluster growth appears to be mainly decahedral with islands of icosahedral and octahedral structures. Our previous studies

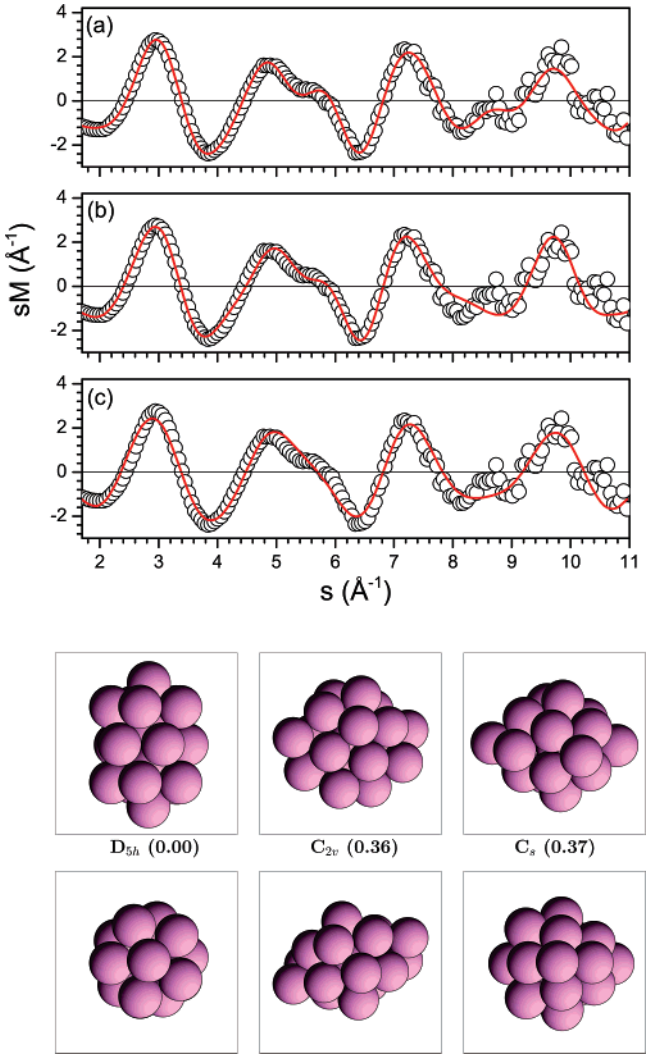

Figure 11. The upper panels show the experimental (circles) and theoretical (full curve) reduced molecular-scattering intensities for three different isomers of Ag_{19}. These are shown in the bottom from the side (upper row) and from the top (lower row). Their symmetries are from left to right D_{5h}, C_{2v}, C_s, and their total energies relative to the most stable structure are 0.00, 0.36, and 0.37 eV.

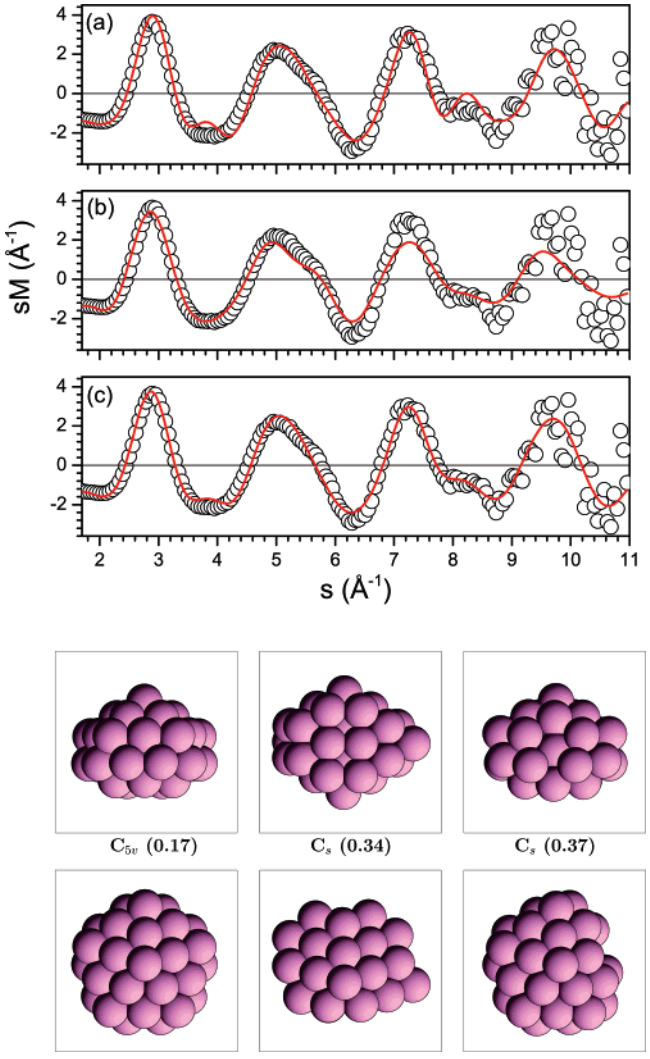

Figure 12. As Figure 11, but for Ag_{38}. The symmetries of the three structures are from left to right C_{5v}, C_s, C_s, and their energies relative to the most stable structure are 0.17, 0.34, and 0.37 eV.

on copper and nickel clusters suggested for those an icosahedral cluster growth, whereas gold clusters showed an irregular behavior. This difference could also be recognized in the similarity function of Figure 2, that is, there are significant structural differences between silver clusters and those of other metals. Although the main magic numbers and structures for $N = 19$, 38, 55, 75, and 147 are the same for all metals, only few structures are very similar for silver, copper, and nickel clusters, except for the smallest clusters with N up to around 15.

Finally, the minimal coordination number that is described elsewhere[51,54] can give further information on cluster growth. A lower value, that is, 3 or 4, indicates a growth by deposition of atoms on the cluster surface, while large values point to an insertion of atoms inside of the cluster. This number is shown in Figure 10 as obtained with the two Gupta potentials. With few exceptions, the two potentials yield very similar results. In contrast to our findings for copper clusters where we found larger values, low-coordinated structures occur significantly more frequently for Ag_N clusters.

In total, our results suggest a decahedral cluster growth. Moreover, silver clusters are only marginally similar to those of copper, nickel, or gold.

D. Comparison with Trapped Ion Electron Diffraction (TIED) Experiment. In a series of combined experimental and theoretical studies,[16,59] the structures of mass-selected silver cluster cations were probed by TIED experiment performed at a temperature of 100 K. The experimentally obtained scattering intensity was compared to results from theoretical calculations for structures that were locally relaxed using the Turbomole program package. For all cluster sizes, the experimental data was best described by structures containing icosahedral motifs, even for the Ag_{38} and Ag_{79} clusters that often have been assumed to be truncated octahedra.

In this subsection, we shall compare our structures from the nG potential for $N = 19$, 38, 55, 59, 75, and 79 to the experimental results.

For a homoatomic cluster, the theoretical reduced molecular-scattering function sM^{theor} can be approximated as (see for example ref 59)

$$sM^{\text{theor}}(s') = \frac{S_c}{N}\exp\left(\frac{-L^2 s'^2}{2}\right)\sum_i\sum_{j\neq i}\left(\frac{\sin(r_{ij}s')}{r_{ij}}\right) \quad (10)$$

where s is the momentum transfer, and r_{ij} is the distance between atoms i and j. The mean square vibrational amplitude L and the amplitude scaling factor S_c are used together with a scaling

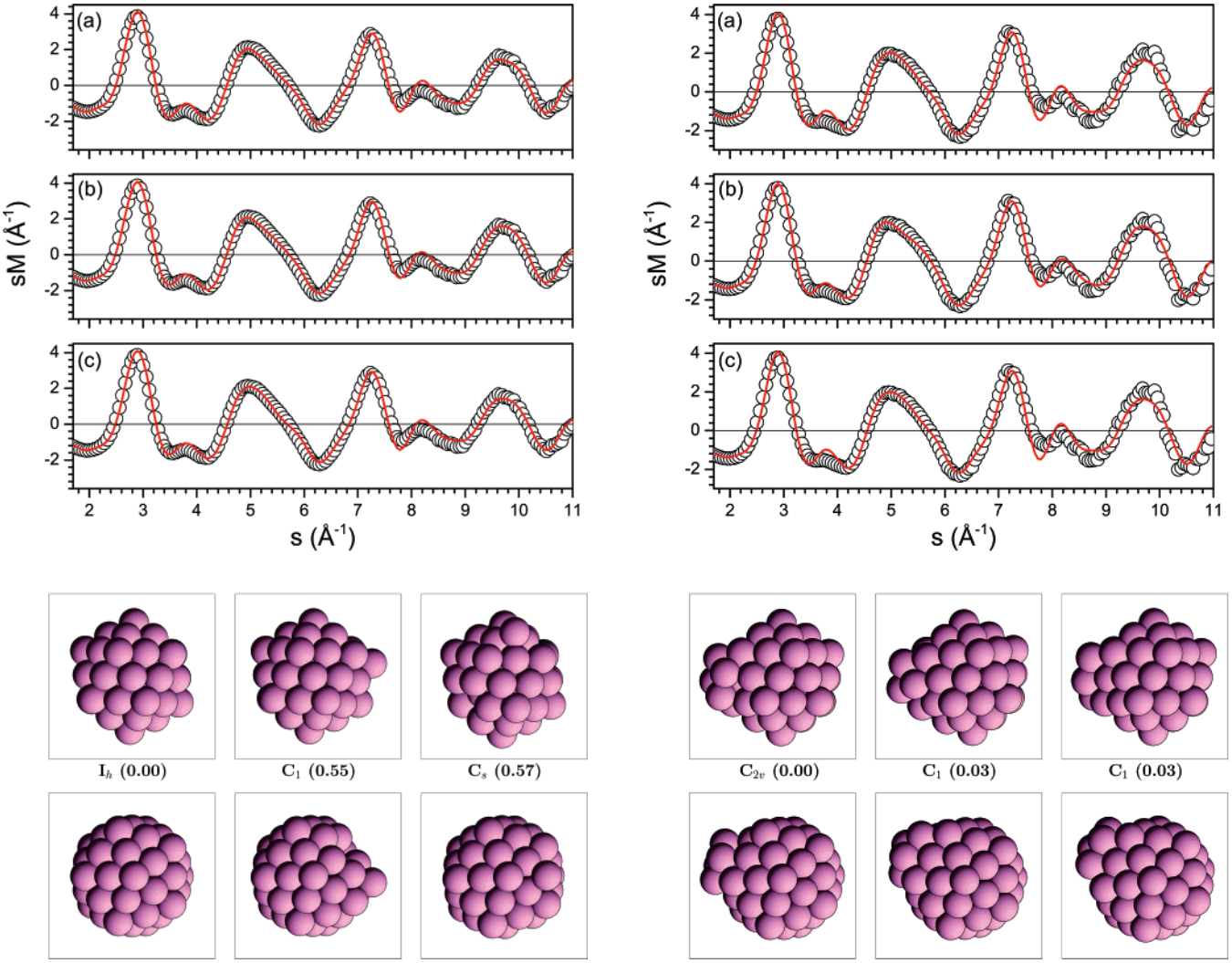

Figure 13. As Figure 11, but for Ag_{55}. The symmetries of the three structures are from left to right I_h, C_1, C_s, and their energies relative to the most stable structure are 0.00, 0.55, and 0.57 eV.

Figure 14. As Figure 11, but for Ag_{59}. The symmetries of the three structures are from left to right C_{2v}, C_1, C_1, and their energies relative to the most stable structure are 0.00, 0.03, and 0.03 eV.

factor for s, k_s, so that $s' = k_s s$. Usually eq 10 is fitted to the experimental molecular scattering intensity simultaneously with an unspecific background intensity approximated by a flat function of a momentum transfer.[59] Hence, one does not expect an important influence of the background intensity function in the fitting procedure. To determine the values of the parameters L, S_c, and k_s we performed a χ^2 fit on the experimental data (kindly provided by Dr. Detlef Schooss, Forschungszentrum Karlsruhe, Germany). The calculated scattering intensities of our three best-fitting structures for each cluster size are shown in Figures 11, 12, 13, 14, 15, and 16.Some disagreements between our results and those of experiment, may be thought to be connected with the following two facts. First, we consider neutral systems, whereas ions are studied in the experiment. For small gold clusters, it has been found that the structures of positively and negatively charged clusters are different.[60] Second, the theoretical molecular-scattering curves in our study have been plotted in each case for a single isomer. However, an experimental diffraction pattern results from averaging over about 10^5 mass-selected clusters and contributions of lowest-energy isomers (or even of an ensemble of low-energy isomers) to the diffraction pattern at the finite experimental temperature of about 100 K may be important if the group of isomers have almost the same total energies. The latter point could be only essential for clusters with low symmetry.

For Ag_{19} the structure that shows the best agreement with the experimental data is the double icosahedron, followed by the low-symmetrical C_{2v} structure. Our third isomer with partly octahedral construction gives a poor description of the experimental results. It is interesting to observe that most semiempirical potentials including the many-body Gupta potential predict the global minimum structure to be a double icosahedron with D_{5h} symmetry. On the other hand, the density functional results in ref 59 found that this structure is 0.38 eV higher in energy than a distorted icosahedron capped with six atoms. In our study, the difference between the first and the second lowest-lying isomers is 0.36 eV. Both structures provide a good reproduction of the experimental results (taking into account that several fitting parameters are involved) so that the comparison is not able unambiguously to distinguish between the two structures.

Many studies have assigned a truncated octahedral symmetry to the Ag_{38} cluster with, however, structures of icosahedral symmetry and disordered structures close in energy. Our results predict an energy gap of 0.17 eV between the fcc global minimum and the next isomer, which has icosahedral structure with C_{5v} symmetry. The fcc structure, according to ref 59 and our calculations, describes very poorly the experiment and is not presented here. For the energetically next isomer (of C_{5v} symmetry), a good agreement with the experimental results was

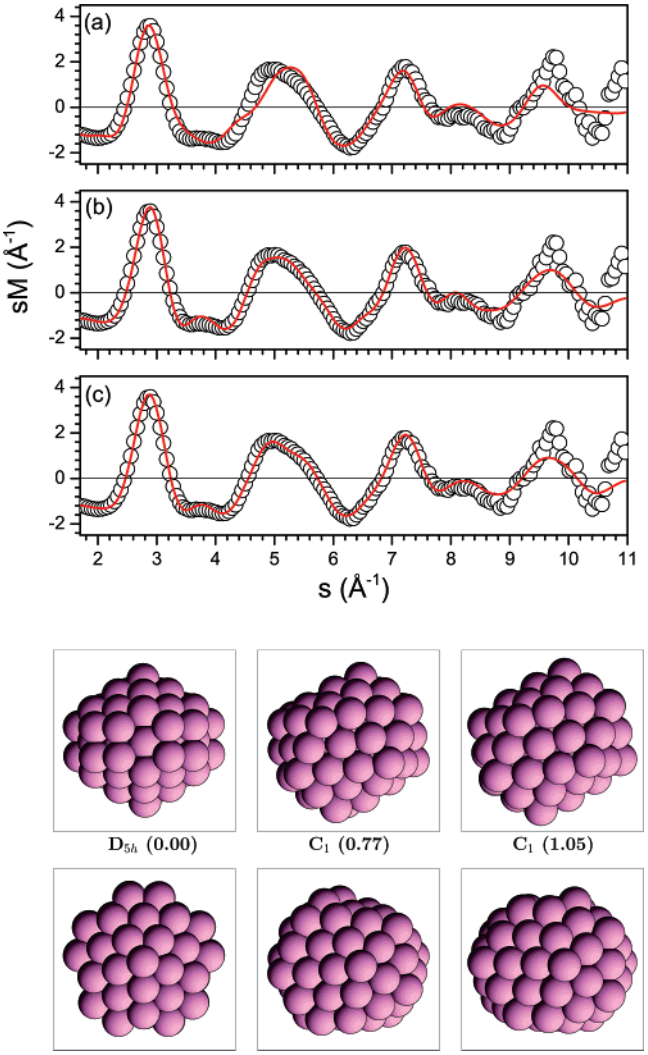

Figure 15. As Figure 11, but for Ag_{75}. The symmetries of the three structures are from left to right D_{5h}, C_1, C_1, and their energies relative to the most stable structure are 0.00, 0.77, and 1.05 eV.

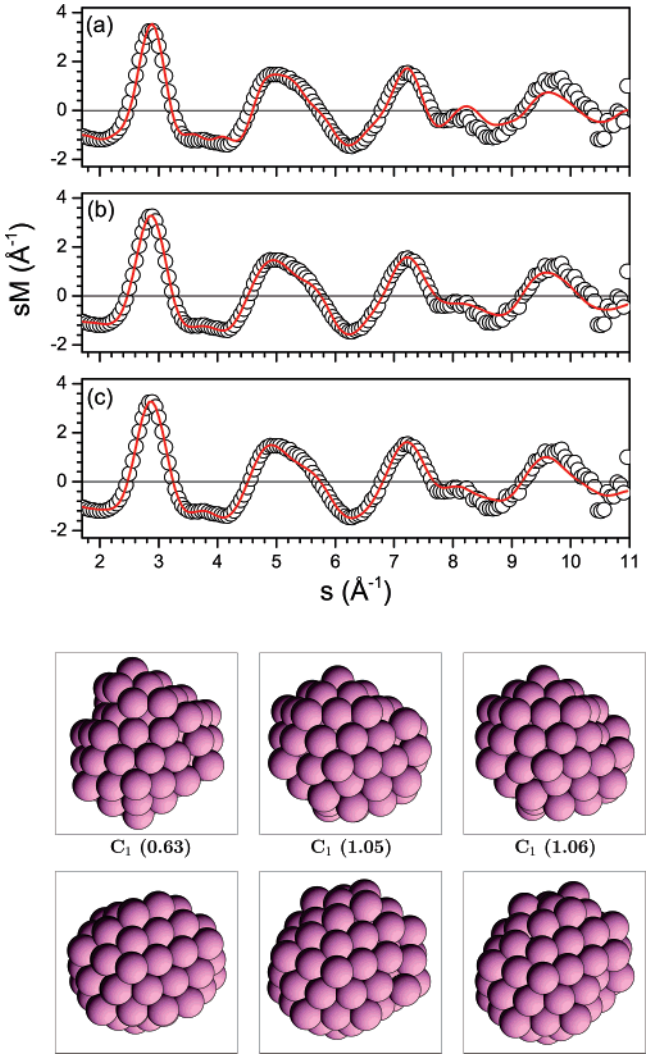

Figure 16. As Figure 11, but for Ag_{79}. The symmetries of the three structures are all C_1, and their energies relative to the most stable structure are 0.63, 1.05, and 1.06 eV.

reported in ref 59. This structure together with two isomers of higher energy are presented in Figure 12. The second and third structures were obtained by the removal of 17 atoms from the icosahedral Ag_{55} cluster and optimization of the resulting structures. All structures describe very well the experimental scattering intensities, supporting a suggestion[16] that the ground state of Ag_{38} is most probably not a single structure, but rather a mixture of low-energy icosahedral isomers.

For Ag_{55} and Ag_{59}, all three lowest-lying isomers give a very good description of the experimental data. Many experimental and theoretical studies have identified the icosahedron as the structure of the global minimum for Ag_{55}. Moreover, this cluster is particularly stable. The second isomer is separated with more than 0.5 eV from the ground state and differs from the icosahedron only by the rearrangement of one atom. Here, cuboctahedral and decahedral structures can be discarded, because according to the *n*G calculations the decahedral Ag_{55} cluster lies 0.93 eV higher in energy than the icosahedron and reproduces very poorly the experimental results, and the cuboctahedron was found to be unstable with this potential. For Ag_{59}, the small structural differences between the three isomers cannot be observed in the calculated scattering intensities. Instead, we can only conclude that for all considered systems, clusters with icosahedral motifs lead to the best agreement with the experimental findings.

Our optimized structures for Ag_{75} and Ag_{79} correspond to a Marks decahedron and a truncated octahedron, respectively. The Marks decahedron describes relatively well the experimental data, showing only one extra shoulder at 4.8 Å^{-1}. This deviation led to the exclusion of this structure in ref 59. In our study, this structure is followed energetically by two decahedral isomers with an energy separation of 0.36 and 0.37 eV from the decahedron, respectively. The same is the situation for the Ag_{79} cluster where the octahedral minimum lies 0.9 eV below the next two isomers that also have octahedral construction. It is, accordingly, clear that the icosahedral isomers will have significantly higher energy than the global minima according to this potential. Furthermore, according to ref 59, cuboctahedral isomers are not observed in experiment for this cluster size. On the other hand, our energetically lowest structure describes very poorly the experimental data and is not shown here. By explicitly including structures with icosahedral symmetry, it was possible to obtain a good agreement with the experimental data, although these structures are energetically unfavorable.

The most important finding of this section is that icosahedral isomers describe best the experimental scattering intensities. The bulk octahedral construction is not preferred, that is, these clusters cannot be considered as being fragments of the large crystal, but are unique systems.

IV. Conclusions

We have presented the results of an unbiased structure optimization study for Ag_N clusters with N up to 150 atoms using two different many-body Gupta potentials. With up to 60 atoms, an energetic and structural comparison was made to independent results from two EAM approaches. Although the small silver clusters obtained with all potentials in general are very similar, significant structural differences occur when looking at the details. These differences show up already at Ag_{15}. However, often an interchange of energetic low-lying isomers was often the reason for the different structures from different potentials. On the other hand, all the potentials we have studied are based on considerations from the infinite, metallic system. Therefore, for the absolutely smallest clusters a comparison with results from calculations that explicitly include electronic degrees of freedom showed significant differences. We suggest that first for clusters with roughly 50 atoms the approximate potentials are becoming more accurate.

Assuming that similar inaccuracies are introduced when considering the same cluster sizes with the same method but for different metals, we could compare our results for silver clusters with those for nickel, copper, and gold clusters. It turned out that copper clusters are those that are most similar to silver clusters, and gold clusters the most different ones, with nickel clusters lying in between.

The similarity functions and the minimal coordination numbers indicated a complicated growth, especially at $N = 31-42$, $N = 62$, 80, 97, 117, and 140 atoms, where significant structural changes take place. The cluster growth is predominantly decahedral with islands of icosahedral and fcc structures, in contrast to the results for copper and nickel clusters, where the main structural motif was the icosahedral construction.

However, a comparison to the experimental scattering intensities unambiguously shows that icosahedral structures are those that are observed. Therefore, here the approximate potentials for silver seem to have a deficit, although it cannot completely be excluded that the fact that the experimentally studied systems are charged may lead to different structures.

Acknowledgment. This work was supported by the DFG through the SFB 277 and through project Sp 439/14-1. We are very grateful to Dr. Detlef Schooss, Forschungszentrum Karlsruhe, Germany, for providing the experimental data of scattering intensities from the TIED experiments and to Dr. Julius Jellinek, Argonne National Laboratory, U.S.A., for his structural data on Ag_N clusters.

References and Notes

(1) Baletto, F.; Ferrando, R. *Rev. Mod. Phys.* **2005**, *77*, 371.
(2) Jackschath, C.; Rabin, I.; Schulze, W. *Ber. Bunsen-Ges. Phys. Chem.* **1992**, *96*, 1200.
(3) Jackschath, C.; Rabin, I.; Schulze, W. *Z. Phys. D* **1992**, *22*, 517.
(4) Alameddin, G.; Hunter, J.; Cameron, D.; Kappes, M. M. *Chem. Phys. Lett.* **1992**, *192*, 122.
(5) Bromann, K.; Félix, C.; Brune, H.; Harbich, W.; Monot, R.; Buttet, J.; Kern, K. *Science* **1996**, *274*, 956.
(6) Fedrigo, S.; Harbich, W.; Buttet, J. *Phys. Rev. B* **1998**, *58*, 7428.
(7) Yeadon, M.; Ghaly, M.; Yang, J. C.; Averback, R. S.; Gibson, J. M. *Appl. Phys. Lett.* **1998**, *73*, 3208.
(8) Carroll, S. J.; Hall, S. G.; Palmer, R. E.; Smith, R. *Phys. Rev. Lett.* **1998**, *81*, 3715.
(9) Krückeberg, S.; Dietrich, G.; Lützenkirchen, K.; Schweikhard, L.; Walther, C.; Ziegler, J. *J. Chem. Phys.* **1999**, *110*, 7216.
(10) Busolt, U.; Cottancin, E.; Röhr, H.; Socaciu, L.; Leisner, T.; Wöste, L. *Appl. Phys. B* **1999**, *68*, 453.
(11) Shi, Y.; Spasov, V. A.; Ervin, K. M. *J. Chem. Phys.* **1999**, *111*, 938.
(12) Hövel, H. *Appl. Phys. A* **2001**, *72*, 295.
(13) Reinert, F.; Nicolay, G.; Schmidt, S.; Ehm, D.; Hüfner, S. *Phys. Rev. B* **2001**, *63*, 115415.
(14) Palmer, R. E.; Pratontep, S.; Boyen, H.-G. *Nat. Mater.* **2003**, *2*, 443.
(15) Häkkinen, H.; Moseler, M.; Kostko, O.; Morgner, N.; Hoffmann, M. A.; v. Issendorff, B. *Phys. Rev. Lett.* **2004**, *93*, 093401.
(16) Xing, X.; Danell, R. M.; Garzón, I. L.; Michaelian, K.; Blom, M. N.; Burns, M. M.; Parks, J. H. *Phys. Rev. B* **2005**, *72*, 081405(R).
(17) Fielicke, A.; Rabin, I.; Meijer, G. *J. Phys. Chem. A* **2006**, *110*, 8060.
(18) Haslett, T. L.; Bosnick, K. A.; Moskovits, M. *J. Chem. Phys.* **1998**, *108*, 3453.
(19) Liu, Z. F.; Yim, W. L.; Tse, J. S.; Hafner, J. *Eur. Phys. J. D* **2000**, *10*, 105.
(20) Bonačić-Koutecky, V.; Veyret, V.; Mitrić, R. *J. Chem. Phys.* **2001**, *115*, 10450.
(21) Häkkinen, H.; Moseler, M.; Landman, U. *Phys. Rev. Lett.* **2002**, *89*, 033401.
(22) Huda, M. N.; Ray, A. K. *Phys. Rev. A* **2003**, *67*, 013201.
(23) Agrawal, B. K.; Agrawal, S.; Srivastava, P.; Singh, S. *J. Nanopart. Res.* **2004**, *6*, 363.
(24) Wang, Y.; Gong, X. G. *Eur. Phys. J. D* **2005**, *34*, 19.
(25) Idrobo, J. C.; Öğüt, S.; Jellinek, J. *Phys. Rev. B* **2005**, *72*, 085445.
(26) Pereiro, M.; Baldomir, D. *Phys. Rev. A* **2007**, *75*, 033202.
(27) Zhao, J.; Luo, Y.; Wang, G. *Eur. Phys. J. D* **2001**, *14*, 309.
(28) de Heer, W. A. *Rev. Mod. Phys.* **1993**, *65*, 611.
(29) Brack, M. *Rev. Mod. Phys.* **1993**, *65*, 677.
(30) Yang, M.; Jackson, K. A.; Jellinek, J. *J. Chem. Phys.* **2006**, *125*, 144308.
(31) Massobrio, C.; Blandin, P. *Phys. Rev. B* **1993**, *47*, 13687.
(32) Vandoni, G.; Félix, C.; Massobrio, C. *Phys. Rev. B* **1996**, *54*, 1553.
(33) Nacer, B.; Massobrio, C.; Félix, C. *Phys. Rev. B* **1997**, *56*, 10590.
(34) Massobrio, C. *J. Phys. Chem. B* **1998**, *102*, 4374.
(35) Arslan, H.; Güven, M. H. *New J. Phys.* **2005**, *7*, 60.
(36) Rey, C.; Gallego, L. J.; García-Rodeja, J.; Alonso, J. A.; Iñiguez, M. P. *Phys. Rev. B* **1993**, *48*, 8253.
(37) García-Rodeja, J.; Rey, C.; Gallego, L. J.; Alonso, J. A. *Phys. Rev. B* **1994**, *49*, 8495.
(38) García González, L.; Montejano-Carrizales, J. M. *Phys. Status Solidi A* **2000**, *220*, 357.
(39) Baletto, F.; Mottet, C.; Ferrando, R. *Phys. Rev. Lett.* **2000**, *84*, 5544.
(40) Baletto, F.; Mottet, C.; Ferrando, R. *Phys. Rev. B* **2001**, *63*, 155408.
(41) Baletto, F.; Ferrando, R.; Fortunelli, A.; Montalenti, F.; Mottet, C. *J. Chem. Phys.* **2002**, *116*, 3856.
(42) Calvo, F.; Doye, J. P. K. *Phys. Rev. B* **2004**, *69*, 125414.
(43) Michaelian, K.; Réndon, N.; Garzón, I. L. *Phys. Rev. B* **1999**, *60*, 2000.
(44) Doye, J. P. K.; Wales, D. J. *New J. Chem.* **1998**, 733.
(45) Shao, X.; Liu, X.; Cai, W. *J. Chem. Theory Comput.* **2005**, *1*, 762.
(46) Gupta, R. P. *Phys. Rev. B* **1981**, *23*, 6265.
(47) Rosato, V.; Guillope, M.; Legrand, B. *Philos. Mag. A* **1989**, *59*, 321.
(48) Cleri, F.; Rosato, V. *Phys. Rev. B* **1993**, *48*, 22.
(49) Daw, M. S.; Baskes, M. I. *Phys. Rev. Lett.* **1983**, *50*, 1285.
(50) Voter, A. F.; Chen, S. P. In *Characterization of Defects in Materials*, Materials Research Society Symposia Proceedings No. 82, Pittsburgh, PA, 1987; Siegal, R. W., Weertman, J. R., Sinclair, R., Eds.; Materials Research Society: Pittsburgh, PA, p. 175.
(51) Grigoryan, V. G.; Springborg, M. *Phys. Rev. B* **2004**, *70*, 205415.
(52) Simard, B.; Hackett, P. A.; James, A. M.; Langridge-Smith, P. R. R. *Chem. Phys. Lett.* **1991**, *186*, 415.
(53) Beutel, V.; Krämer, H.-G.; Bhale, G. L.; Kuhn, M.; Weyers, K.; Demtröder, W. *J. Chem. Phys.* **1993**, *98*, 2699.
(54) Grigoryan, V. G.; Alamanova, D.; Springborg, M. *Phys. Rev. B* **2006**, *73*, 115415.
(55) Alamanova, D.; Grigoryan, V. G.; Springborg, M. *Z. Phys. Chem.* **2006**, *220*, 811.
(56) Grigoryan, V. G.; Alamanova, D.; Springborg, M. *Eur. Phys. J. D* **2005**, **34**, 187.
(57) Jennison, D. R.; Schultz, P. A.; Sears, M. P. *J. Chem. Phys.* **1997**, *106*, 1856.
(58) Jellinek, J. private communication, 2007.
(59) Blom, M. N.; Schooss, D.; Stairs, J.; Kappes, M. M. *J. Chem. Phys.* **2006**, *124*, 244308.
(60) Häkkinen, H.; Yoon, B.; Landman, U.; Li, X.; Zhai, H.-J.; Wang, L.-S. *J. Phys. Chem. A* **2003**, *107*, 6168.